Supplemental Material can be found at:
http://www.mcponline.org/cgi/content/full/M700085-MCP200
/DC1

Proteomics Analysis of Cytokine-induced Dysfunction and Death in Insulin-producing INS-1E Cells

NEW INSIGHTS INTO THE PATHWAYS INVOLVED*[S]

Wannes D'Hertog,[a,b] Lut Overbergh,[a,b,c] Kasper Lage,[d] Gabriela Bonfim Ferreira,[a] Michael Maris,[a] Conny Gysemans,[a] Daisy Flamez,[e] Alessandra Kupper Cardozo,[e,f] Gert Van den Bergh,[g] Liliane Schoofs,[h,i] Lut Arckens,[g,i] Yves Moreau,[j] Daniel Aaen Hansen,[d] Decio Laks Eizirik,[e] Ettienne Waelkens,[i,k] and Chantal Mathieu[a]

Cytokines released by islet-infiltrating immune cells play a crucial role in β-cell dysfunction and apoptotic cell death in the pathogenesis of type 1 diabetes and after islet transplantation. RNA studies revealed complex pathways of genes being activated or suppressed during this β-cell attack. The aim of the present study was to analyze protein changes in insulin-producing INS-1E cells exposed to inflammatory cytokines *in vitro* using two-dimensional DIGE. Within two different pH ranges we observed 2214 ± 164 (pH 4–7) and 1641 ± 73 (pH 6–9) spots. Analysis at three different time points (1, 4, and 24 h of cytokine exposure) revealed that the major changes were taking place only after 24 h. At this time point 158 proteins were altered in expression (4.1%, $n = 4$, $p \leq 0.01$) by a combination of interleukin-1β and interferon-γ, whereas only 42 and 23 proteins were altered by either of the cytokines alone, giving rise to 199 distinct differentially expressed spots. Identification of 141 of these by MALDI-TOF/TOF revealed proteins playing a role in insulin secretion, cytoskeleton organization, and protein and RNA metabolism as well as proteins associated with endoplasmic reticulum and oxidative stress/defense. We investigated the interactions of these proteins and discovered a significant interaction network ($p < 1.27e-05$) containing 42 of the identified proteins. This network analysis suggests that proteins of different pathways act coordinately in a β-cell dysfunction/apoptotic β-cell death interactome. In addition the data suggest a central role for chaperones and proteins playing a role in RNA metabolism. As many of these identified proteins are regulated at the protein level or undergo post-translational modifications, a proteomics approach, as performed in this study, is required to provide adequate insight into the mechanisms leading to β-cell dysfunction and apoptosis. The present findings may open new avenues for the understanding and prevention of β-cell loss in type 1 diabetes. *Molecular & Cellular Proteomics 6:2180–2199, 2007.*

The hallmark of type 1 diabetes is β-cell dysfunction and apoptotic β-cell death mediated by infiltrating immune cells, especially macrophages and T-cells, into the islets of Langerhans. Cytokines, such as interleukin-1β (IL-1β),[1] interferon-γ (IFN-γ), and tumor necrosis factor α, secreted by these immune cells are one of the main causes of β-cell death (1, 2). β-Cells are highly specialized cells primarily oriented toward tightly regulated insulin synthesis and secretion. Because of the high demand of proinsulin/insulin processing, they possess a highly developed endoplasmic reticulum (ER) compartment. The correct folding of proinsulin in this ER compartment is mediated by a specific subset of proteins, the molecular chaperones. Altered expression of several of these

From the [a]Laboratory for Experimental Medicine and Endocrinology, University Hospital Gasthuisberg, Catholic University of Leuven, Herestraat 49, box 902, B-3000 Leuven, Belgium, [d]Centre for Biological Sequence Analysis, BioCentrum-DTU, Technical University of Denmark, Building 208, DK-2800 Lyngby, Denmark, [e]Laboratory for Experimental Medicine, Université Libre de Bruxelles, route de Lennik 808, box CP618, B-1070 Brussels, Belgium, [g]Laboratory of Neuroplasticity and Neuroproteomics and [h]Functional Genomics and Proteomics Research Unit, Catholic University of Leuven, Naamsestraat 59, B-3000 Leuven, Belgium, [i]ProMeta and [k]Laboratory of Biochemistry, University Hospital Gasthuisberg, Catholic University of Leuven, Herestraat 49, box 901, B-3000 Leuven, Belgium, and [j]ESAT-SDC, Department of Electrical Engineering, Catholic University of Leuven, Kasteelpark Arenberg 10, box 2446, B-3001 Heverlee, Belgium

Received, February 27, 2007, and in revised form, September 27, 2007

Published, MCP Papers in Press, October 5, 2007, DOI 10.1074/mcp.M700085-MCP200

[1] The abbreviations used are: IL-1β, interleukin-1β; BiP/GRP78, immunoglobulin heavy chain-binding protein/glucose-regulated protein, 78 kDa; DDX1, DEAD box protein 1; DDX3X, DEAD box protein 3 X-chromosomal; ER, endoplasmic reticulum; hnRNP, heterogeneous nuclear ribonucleoprotein; HSPA8, heat shock 70-kDa protein 8; HSPA9, mortalin; IFN-γ, interferon-γ; NO, nitric oxide; ORP150, oxygen-regulated protein, 150 kDa; PTM, post-translational modification; PRDX, peroxiredoxin; ROS, reactive oxygen species; SOD2, manganese-superoxide dismutase; STAT1, signal transducer and activator of transcription 1; 2D, two-dimensional; 2DE, two-dimensional gel electrophoresis; TXNL1, thioredoxin-like protein 1; BLAST, Basic Local Alignment Search Tool; NCBI, National Center for Biotechnology Information; iHOP, Information Hyperlinked over Proteins.

© 2007 by The American Society for Biochemistry and Molecular Biology, Inc.
This paper is available on line at http://www.mcponline.org

Molecular & Cellular Proteomics

Downloaded from www.mcponline.org by on January 2, 2008

chaperones in response to different stress situations has been associated with the pathogenesis of type 1 and even type 2 diabetes (3).

Not surprisingly, one of the major changes in β-cells upon exposure to inflammatory cytokines is an increased proinsulin/insulin ratio and loss of insulin secretion in response to glucose (4–6). Upon prolonged exposure of the β-cells to cytokines this functional impairment leads to apoptotic β-cell death as shown convincingly by *in vitro* exposure of human or rodent β-cells to cytokines (2, 7, 8). Many studies have been undertaken in an attempt to unravel the pathways involved in cytokine-induced β-cell destruction, revealing that stress response genes, either protective or deleterious for β-cell survival, are induced, whereas several genes related to differentiated β-cell functions are down-regulated (7, 9). Central factors in the regulation of these cytokine-induced genes are nuclear factor κB and signal transducer and activator of transcription 1 (STAT1) (7, 10, 11). The strength of the microarray technique used for the majority of these studies is that it allows analysis of a very large number of genes; however, the technique yields little information on the functional state of the cells as changes in transcript levels are not always reflected at the protein level (12). In addition, many forms of regulation take place at a post-transcriptional level, such as post-translational modifications (PTMs), proper protein folding, and selective proteolytic degradation (13, 14). It is thus crucial to complement cDNA array analysis with a global evaluation of protein expression. Previous proteomics studies have been performed on mechanisms of β-cell death mainly on whole rat islets. Most of these studies made use of classical two-dimensional gel electrophoresis (2DE) and focused on the effects of IL-1β alone on rat islets (15–17). Although these contributed greatly to our current understanding on the mechanisms involved in β-cell death, we believe that the use of other inflammatory stimuli, such as a combination of IL-1β and IFN-γ, will add valuable data improving our knowledge on the mechanisms involved in cytokine-induced β-cell death. Indeed although exposure of purified human or rodent β-cells to IL-1β alone will induce β-cell dysfunction, it is not sufficient to induce apoptosis (2). Combining IL-1β with IFN-γ will induce an extensive level of apoptosis, as reported in human and rodent islets as well as in INS-1E cells, even at relatively low cytokine concentrations. This suggests that IFN-γ signal transduction synergizes with IL-1β signaling to trigger β-cell apoptosis (3).

With the recent advances in differential dye labeling and the introduction of the 2D DIGE technique (18) as well as the development of more sophisticated MS equipment for protein identification, an attractive technology for the quantitative analysis of differences in protein profiles has become available (19, 20). In the present project we investigated by 2D DIGE analysis the complex processes involved in cytokine-induced β-cell death, making use of the rat insulin-producing INS-1E cell line. These are well differentiated cells and have been found to be a stable and reliable β-cell model (21) with a global pattern of cytokine-induced gene expression similar to that observed in primary β-cells (9, 22). The effects of single cytokine treatments as well as a combined treatment with IL-1β and IFN-γ were analyzed, each covering a broad pH range by using an overlap of two different IPG strips (pH 4–7 and 6–9). This allowed us to conclude that, at the concentrations presently used, IL-1β and IFN-γ act synergistically in the induction of apoptosis, concurrent with major alterations in protein levels, as compared with single cytokine treatment alone. Interestingly the minor changes observed in single cytokine treatments point to a protection or adaptation of the INS-1E cells toward the treatment. For the combined treatment, where we were able to identify 119 differentially expressed proteins, the changes are consistent with an induction of the apoptotic cell type. Importantly many of the regulations observed occur at a post-translational level, for instance for the ER chaperones immunoglobulin heavy chain-binding protein/glucose-regulated protein, 78 kDa (BiP/GRP78) and oxygen-regulated protein, 150 kDa (ORP150) and for the heterogeneous nuclear ribonucleoproteins (hnRNPs). A protein interaction analysis of the differentially expressed proteins revealed a significant network ($p < 1.27e-05$) containing 42 of these proteins. These results suggest that many of the pathways involved act in a coordinate way with a central role for molecular chaperones and proteins involved in RNA metabolism.

EXPERIMENTAL PROCEDURES

Cell Culture Conditions—INS-1E cells, a kind gift from Prof. C. Wollheim (Centre Medical Universitaire, Geneva, Switzerland), were cultured in RPMI 1640 medium (Cambrex, Verviers, Belgium) supplemented with 10 mmol/liter HEPES, 10% (v/v) heat-inactivated FCS, 100 units/ml penicillin, 100 μg/ml streptomycin, 1 mmol/liter sodium pyruvate, and 50 μmol/liter β-mercaptoethanol. Cells used for experiments ranged from passage 64 to 70 (21).

Cell Death Analysis and Nitrite Determination—The percentage of living, apoptotic, and necrotic cells was assessed by cell counting. INS-1E cells were cultured in 96-well plates (7500 cells/well). Typically after 24 h of control or cytokine-treatment (10 units/ml IL-1β, 500 units/ml IFN-γ, or the combination of the two cytokines with the same concentrations) cells were incubated for 15 min with propidium iodide (10 μg/ml) and Hoechst HO 342 (20 μg/ml) (23). A minimum of 500 cells was counted in each experimental condition by two researchers counting independently of each other on a Zeiss Axiovert 40 CFL fluorescence microscope (Zeiss, Jena, Germany).

For nitrite determination, 50 μl of culture supernatant was collected after 24 h from the cell cultures for the proteomics experiments (2.5×10^6 cells/100-mm dish). Nitrite determination was performed using Griess reagent as described previously (24), and the concentration was determined spectrophotometrically at 546 nm.

Sample Preparation for 2D DIGE Analysis—INS-1E cells were incubated for 1, 4, and 24 h with 10 units/ml recombinant human IL-1β (a kind gift from Dr. C. W. Reinolds, National Cancer Institute, National Institutes of Health, Bethesda, MD) and 500 units/ml recombinant rat IFN-γ (R&D Systems, Minneapolis, MN). For the 24-h condition, cells were also incubated with individual cytokines using the same concentrations. For each condition, 12.5×10^6 INS-1E cells (2.5×10^6 cells/100-mm dish) were collected. For each time point or treatment

Molecular & Cellular Proteomics

Downloaded from www.mcponline.org by on January 2, 2008

condition quadruplicate experiments were performed, originating from four independent experiments. The cells were washed twice in phosphate-buffered saline and resuspended in 100 μl of lysis buffer (7 M urea, 2 M thiourea, 4% (w/v) CHAPS, 40 mM Tris base, 1% (w/v) DTT, and a mixture of protease inhibitors (Complete protease inhibitor, Roche Diagnostics)). Samples were sonicated (UP50H, Hielscher, Teltow, Germany) five times for 10 s after which they were centrifuged for 13 min at 20,000 × *g* (4 °C) to precipitate all nonsoluble proteins and membrane fractions. The supernatant was desalted by dialysis (PlusOne Mini Dialysis kit, GE Healthcare), and the pH was adjusted to 8.5. Protein concentration was determined using the Bradford assay (25). 50 μg of protein sample was labeled with 200 pmol of Cy3 or Cy5 (two "forward" and two "reverse" gels were made at each time point), whereas 50 μg of pooled internal standard was labeled with 200 pmol of Cy2 (18). The internal standard consisted of a pool of all control and treated samples of all four replicate experiments. The labeling reaction was carried out for 30 min on ice and quenched with 10 mM lysine (15 min on ice). Labeled protein extracts were pooled, and sample loading buffer was added (7 M urea, 2 M thiourea, 4% (w/v) CHAPS, 0.5% (v/v) IPG buffer, and depending on the pH range of the strips, 1% (w/v) DTT for IPG strips pH 4–7 or 1.2% (v/v) Destreak (GE Healthcare) for pH 6–9).

2D DIGE and Gel Imaging—IPG strips (24 cm) were rehydrated overnight in 450 μl of rehydration buffer (7 M urea, 2 M thiourea, 4% (w/v) CHAPS, 0.5% (v/v) IPG buffer, 0.05% (w/v) OrangeG, and either 1% (w/v) DTT (for IPG strips pH 4–7) or 1.2% (w/v) Destreak (for IPG strips pH 6–9)). The pooled samples containing sample loading buffer were loaded onto the rehydrated strips using anodic cup loading and separated according to their isoelectric point on an Ettan IPGphor II manifold. The complete process was tracked using the Ettan IPGphor control software (version 1.01.03) (GE Healthcare). The first dimension was ended when the current reached a stable phase (at ~60 kV-h).

Prior to the second dimension, the strips were equilibrated during two intervals of 15 min each in an equilibration buffer (6 M urea, 30% (v/v) glycerol, 2% (w/v) SDS, and 50 mM Tris-HCl, pH 8.8) containing 1% (w/v) DTT in the first step and 4% (w/v) iodoacetamide and 0.02% bromphenol blue in the second step. Equilibrated strips were placed on top of 12.5% SDS-polyacrylamide gel and separated on an Ettan DaltSix system (GE Healthcare).

Scanning of the gels was performed using a Typhoon 9400 (GE Healthcare) at 100-μm pixel size. Prior to analysis with the DeCyder™ Version 6.5 software, gel images were cropped using ImageQuant TL. Spot detection and matching was performed automatically using the "Batch Processor" module of the DeCyder Version 6.5 software followed by careful manual rematching of wrongly matched spots or unmatched spots. The 12 spot maps corresponding to the four gels from each time point and each pH range were used to calculate average abundance.

Spot Digestion and Protein Identification by MALDI-TOF/TOF Analysis—For spot picking, two preparative gels for each pH range were run (350 μg of protein lysate each). First and second dimension runs were performed as described above except that CyDye labeling was omitted. Glass plates were pretreated with BindSilane, and two reference markers were applied to enable automatic picking. The gels were poststained using Deep Purple (GE Healthcare). Matching with the analytical gels was performed using the biological variation analysis module of the DeCyder Version 6.5 software. A pick list was generated and exported into the Spot Picker Version 1.20 software that controls the Ettan Spot Picker (GE Healthcare).

Spots were picked in MilliQ water, transferred to 100 μl of fixation solution (50% (v/v) methanol, 5% (v/v) acetic acid, and 45% (v/v) MilliQ) and rinsed three times with MilliQ water and three times with ACN (LC-MS quality, CHROMASOLV®, Sigma-Aldrich). The gels were hydrated in a 100 mM NH_4HCO_3 solution for 10 min followed by a dehydration step in 100% ACN for 10 min with vigorous vortexing. This step was repeated twice prior to dehydrating the gel pieces in a SpeedVac.

Gel pieces were rehydrated in digestion buffer (50 mM NH_4HCO_3 and 5 mM $CaCl_2$) containing 5 ng/μl modified trypsin (Promega, Madison, WI) and incubated overnight at 37 °C. The resulting peptides were extracted out of the gel plugs in four steps: once with 50 mM NH_4HCO_3, twice with 50% (v/v) ACN and 5% (v/v) formic acid, and once with 95% ACN and 5% formic acid (30 min each). Supernatants were dried in a SpeedVac.

Upon concentrating and desalting the tryptic fragments using Millipore C_{18} ZipTips, the samples were mixed in a 1:1 (v/v) ratio with α-cyano-4-hydroxycinnamic acid matrix (saturated solution in 50% ACN and 2.5% TFA in HPLC water), spotted onto the MALDI target plate, and allowed to air dry. MS/MS analyses were performed on a 4800 MALDI-TOF/TOF instrument (Applied Biosystems, Foster City, CA). The instrument was calibrated with Applied Biosystems Calibration Mixture 1. Measurements were taken in the positive ion mode between 900 and 3000 *m/z*. Sequences were automatically acquired by scanning first in MS mode and selecting the 15 most intense ions for MS/MS using an exclusion list of peaks arising from tryptic autodigestion. Air was used as the collision gas, whereas the collision energy was adapted automatically. Data interpretation was carried out using the GPS Explorer software (Version 3.5), and database searching was carried out using the Mascot program (Version 2.0.00). Because all experiments were performed on rat INS-1E cells, MS/MS searches were conducted with the following settings: NCBI (taxonomy set on *Rattus*, 33,734 protein entries) and MSDB (Mass Spectrometry Protein Sequence Database) (taxonomy set on Rodentia, 88,439 protein entries) as database, MS/MS tolerance for precursor and fragment ions between 0.2 and 1 Da depending on the sample, methionine oxidation as variable modification, and carbamidomethylation of cysteine as fixed modification. As enzyme, trypsin was selected, and a maximum of one missed cleavage was allowed. Using these parameters the probability-based MOWSE (Molecular Weight Search) scores greater than the given cutoff value for MS/MS fragmentation data were taken as significant ($p < 0.05$).

For protein identifications where no hit was found in the rat databases, protein identity was based on comparison with the orthologous mouse sequence because the mouse genome is better annotated compared with the rat genome. In these cases the number of identical amino acids is indicated for each peptide (Supplemental Table 1). For all identified proteins, each sequenced peptide was individually aligned using BLAST (26). For protein identifications where all the individual peptides completely matched to more than one Swiss-Prot database accession number/protein name, both protein sequences were aligned using BLAST (26). If this alignment resulted in 100% sequence identity, thus pointing to a single protein present in the database under different names/accession numbers, the Swiss-Prot accession number of the entry with the best description is consistently given in the first place to eliminate redundancy. For completeness also the second accession number is reported (Supplemental Table 1). For peptides matching to different isoforms or to multiple members of a protein family, the following criteria were used for selecting which one to report. 1) If at least one of the identified peptides matched exclusively to a specific isoform or protein member, this protein isoform/member could be identified unambiguously. 2) The experimental molecular weight and pI obtained from the 2DE gel was compared with the theoretical molecular weight and pI of the different isoforms/protein members. In case no single protein could be ruled out based on these criteria or possibly more than one member of the protein group could be present in a single spot, the different names/accession numbers are reported, including the percent identity between them (Supplemental Table 1).

Molecular & Cellular Proteomics

Downloaded from www.mcponline.org by on January 2, 2008

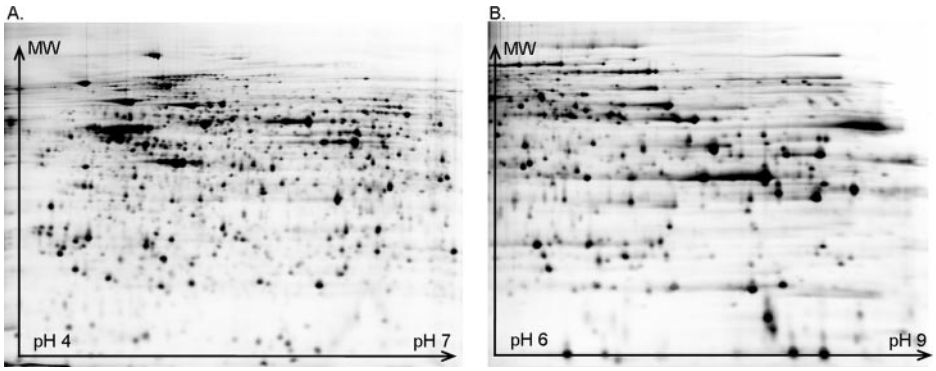


FIG. 1. **Grayscale images of 2D DIGE gels from INS-1E cells, pH range 4–7 (*A*) and pH range 6–9 (*B*).** Each gel contains 50 μg of protein lysate from control cells, 50 μg from IL-1β/IFN-γ-treated cells (labeled with Cy3 or Cy5), and 50 μg of pooled internal standard. One representative experiment of four is shown.

Constructing a Human Protein Interaction Network—We constructed a human protein interaction network as reported recently (27, 28). Data were downloaded from MINT 48, BIND 49, IntAct 50, KEGG (Kyoto Encyclopedia of Genes and Genomes), and Reactome. To increase the coverage of interactions, interolog data 53 (the transfer of protein interactions between orthologous protein pairs in different organisms) were included. Interactions were transferred from 17 eukaryotic organisms and added to the network. Orthology was assigned using the Inparanoid database 55 using stringent thresholds. The statistical significance of the networks was estimated using a randomization scheme in which networks were generated from random input sets of the same size as in the present experiment. We performed 1000 randomizations from which we derived a probability distribution that was used to calculate the significance of the networks in this study (28).

Statistical Analysis—For all experiments the paired Student's *t* test was used. To analyze differences in protein levels, the DeCyder Version 6.5 software was used, and a *p* value of less than or equal to 0.01 was considered statistically significant.

RESULTS

Effects of Cytokines on Cell Viability and Nitric Oxide Production—INS-1E cells were exposed for 24 h with IL-1β (10 units/ml), IFN-γ (500 units/ml), or the combination of both cytokines. In parallel to the cell culture experiments performed for proteomics analysis, we investigated the effects of the cytokines on cell viability and nitric oxide (NO) production. As reported previously (9), only a minor increase in the proportion of apoptotic cells was observed with IL-1β (from 1.88 ± 0.83 to 5.40 ± 2.09%, $p < 0.005$, $n = 4$) or IFN-γ alone (from 1.88 ± 0.83 to 7.10 ± 2.09%, $p < 0.05$, $n = 4$), whereas a synergistic effect on apoptosis was seen in the combination-treated cells (from 1.88 ± 0.83 to 21.42 ± 4.93%, $p < 0.0005$, $n = 4$). No significant alterations in the proportion of necrotic cells were observed. In parallel with this increase in apoptosis, NO production increased from 29.31 ± 20.7 pmol of nitrite/10^4 cells in control cells to 624.38 pmol of nitrite/10^4 cells in IL-1β-exposed cells or to 809.85 ± 170.7 pmol of nitrite/10^4 cells in IL-1β + IFN-γ-exposed cells ($p < 0.001$, $n = 4$). For IFN-γ alone, no significant rise in NO production was detected (35.27 ± 12.9 pmol of nitrite/10^4 cells). These findings are in accordance with previously performed studies investigating alterations in mRNA levels in cytokine-induced INS-1E cells under similar conditions (9).

Differential Proteomic Profile of Cytokine-exposed INS-1E Cells—Proteomic profiles of cytokine-exposed INS-1E cells were determined at two early time points (1 and 4 h) and at one late time point after cytokine induction (24 h) in an attempt to distinguish between early and late effects induced by IL-1β and IFN-γ. In addition, after 24 h of incubation, also the effects of IL-1β and IFN-γ alone were investigated. For each of these conditions quadruplicate experiments were performed at two different pH ranges, comparing cytokine-exposed with non-exposed control INS-1E cells. In the pH 4–7 range, 2328 ± 151 spots could be matched for IL-1β and IFN-γ alone, and 2214 ± 164 spots could be matched for the combination of IL-1β and IFN-γ. Similarly for the pH 6–9 range a total of 1821 ± 184 spots were matched for IL-1β alone and IFN-γ alone, and 1641 ± 73 spots were matched for the combination. In the pH 4–7 range 31, 23, and 116 spots were observed as differentially expressed after 24-h incubation with IL-1β alone, IFN-γ alone, or IL-1β + IFN-γ, respectively ($p \leq 0.01$) (Fig. 1*A* and Supplemental Fig. 1). In addition, only 1 and 19 spots were differentially expressed after IL-1β + IFN-γ treatment at the early time points of 1 and 4 h of incubation, respectively. Because some of these spots were differential in different treatment conditions or at different time points, a total of 159 spots was observed to be differential. For the pH range 6–9, 11, 0, and 30 spots were observed as differentially expressed after treatment with IL-1β alone, IFN-γ alone, and IL-1β + IFN-γ, respectively ($p \leq 0.01$, 24 h). For the early time points no spots were differentially expressed after 1 h of incubation, and only two spots were differentially expressed after 4 h of incubation with the combination treatment ($p \leq 0.01$). Taken together, a total of 40 different differential spots were observed when analyzing this pH range (Fig. 1*B* and Supplemental Fig. 2).

Identification and Classification of Differentially Expressed Proteins—We obtained the following results from our 2D DIGE experiments for the combination of IL-1β + IFN-γ. Of a total of 199 differentially expressed spots, we were able to identify 141 spots (70.9%) by MALDI-TOF/TOF, corresponding to 92 different proteins. Of note, 12 of these spots were found to contain two proteins. Therefore, it is at present not possible to conclude which protein in the spot actually changed expression upon cytokine treatment. Further analysis using narrow

Downloaded from www.mcponline.org by on January 2, 2008

pH range zoom strips could tackle this problem. The identified proteins were grouped in different functional classes: 1) metabolism; 2) protein synthesis, modification, and secretion; 3) ionic channels, ion transporters, and related proteins; 4) processing of peptides and neurotransmitters; 5) cell adhesion, cytoskeleton, and related genes; 6) RNA synthesis/turnover; 7) cell cycle and related genes; 8) defense/repair; 9) apoptosis/endoplasmic reticulum stress-related; and 10) miscellaneous (Tables I–IV). The same functional classes were used in our previous microarray analysis (9). The complete list of identified proteins is shown in Tables I–IV and includes information on the -fold regulation, Swiss-Prot accession number, number of identified peptide sequences, number of unique peptides, and percent sequence coverage. Additional information is shown in Supplemental Table 1. Although the majority of protein identifications are based on multiple peptide sequences, three identifications are single peptide-based protein identifications. For these latter proteins the peptide sequence, precursor *m/z* and charge ratio, and the score/Expect value are shown in Table V, and the annotated MS/MS spectra are shown in Supplemental Fig. 3. The identified proteins play a role in many different pathways, such as insulin biosynthesis (summarized in Fig. 2), energy metabolism (summarized in Fig. 3), cytoskeleton reorganization (summarized in Fig. 4) (29–33), RNA metabolism (such as hnRNP H, hnRNP K, DEAD box protein 1 (DDX1), DEAD box protein 3 X-chromosomal (DD3X3)), oxidative stress (such as manganese-superoxide dismutase (SOD2), peroxiredoxin-1 (PRDX1), and peroxiredoxin-3 (PRDX3)), and molecular chaperones (BiP/GRP78, ORP150, heat shock 70-kDa protein 8 (HSPA8), and mortalin (HSPA9)).

Interestingly 34.8% of the identified proteins are represented in more than one spot, suggesting that they are undergoing PTM (indicated in Tables I–IV). The two ER-residing chaperones, BiP/GRP78 and ORP150, for example, are present in a train of spots suggestive for phosphorylation. For both chaperones the unmodified form is down-regulated by cytokine treatment ($p < 0.01$ for BiP/GRP78 and $p < 0.05$ for ORP150), whereas the modified forms, although not all of them at a significant level, are induced by cytokine treatment (Fig. 5). Also HSPA8, a cytosolic chaperone, was represented by three different isoforms, which were all down-regulated upon cytokine treatment. The position of the isoforms in the gel suggests that one of them is phosphorylated (spot 931 compared with spot 922 (native form)), whereas the other is undergoing another PTM or possibly alternative splicing (spot 971). The fourth differentially expressed chaperone, the mitochondrial HSPA9, was observed in two spots. The isoform in spot 1013 (pH 4–7) was induced by cytokine treatment, whereas the second isoform (spot 994 (pH 4–7)) co-localized with another protein, *i.e.* the neuroendocrine convertase 1 (PCSK1). Therefore it is difficult at present to make a conclusion on the possible up-regulation of this second isoform. A better separation of these spots, *e.g.* by using narrow range IPG strips, is necessary to allow conclusions on the differential expression of either of these proteins.

Another protein undergoing PTM is the cytoplasmic PRDX1 (spot 2014, pH 6–9), which was strongly induced (7.6-fold, $p \leq 0.01$), whereas an isoform of PRDX1 (spot 1975, pH 6–9) was down-regulated (2.7-fold, $p \leq 0.01$). Another group of proteins prone to PTM are the hnRNPs. Two different members have been identified (hnRNP H1 and hnRNP K), represented in a total of eight different spots; all were down-regulated ($p \leq 0.01$). Especially hnRNP K seems to be prone to PTMs because six different spots contained this protein. These can be divided into two distinct groups of phosphorylated isoforms, with molecular mass of ~70 and 51 kDa, respectively. Also of note, for PCSK1 and PCSK2, two and six isoforms were identified, respectively, all with the same molecular weight and all significantly down-regulated ($p \leq 0.01$).

Upon exposure to individual cytokines, we were able to identify 38 (30 and 17 identifications for IL-1β and IFN-γ, respectively) proteins of a total of 57 (40 and 23 spots for IL-1β and IFN-γ, respectively) differentially expressed proteins (75% of the spots identified for IL-1β and 74% of the spots identified for IFN-γ). These are listed in Tables III and IV, classified using the same functional groups as above. An important subset of proteins identified in IL-1β-exposed cells were proteins involved in metabolism, whereas the main group of proteins altered by IFN-γ plays a role in defense and repair pathways. Of interest, more than half of the proteins identified in the single cytokine condition were not altered significantly in combination-exposed cells. In addition, more than 80 additional proteins were identified in combination-exposed cells compared with single cytokine-exposed cells, confirming the synergistic nature of the combined cytokine exposure.

Network Analysis—Because the majority of changes in protein profile were observed by treatment with the combination of IL-1β and IFN-γ, and this after 24 h of stimulation, concurrent with a major increase in apoptosis, this condition was chosen for further network analysis. Considering that most proteins do not act as single entities but work together in networks, we analyzed the interactions between the proteins identified in this work. This allowed us to examine whether the differentially expressed proteins form one or more functional pathways and to place them in a framework of cellular systems. For this purpose the identified proteins were placed in a protein interaction network recently developed by us (27, 28). This analysis revealed that 42 of the differentially expressed proteins identified constitute a significant interaction network ($p < 1.27e-05$). This suggests extensive cross-talk between the different proteins and the pathways in which they are involved (Fig. 6 and Supplemental Material 3) with some proteins such as the chaperones BiP/GRP78, HSPA8, and HSPA9 and the RNA synthesis/turnover proteins placed at the center of different networks.

Molecular & Cellular Proteomics

Downloaded from www.mcponline.org by on January 2, 2008

TABLE I

Identification of proteins with an altered protein expression level upon 4 h of IL-1β and IFN-γ incubation in INS-1E cells

pH	Spot no.	Full protein name	Protein name[a]	Swiss-Prot accession no.[b]	-Fold regulation[c]	No. peptides sequenced[d]	No. of unique peptides[e]	Sequence coverage
								%
1. Metabolism								
Up-regulated								
4–7	1443	Aldehyde dehydrogenase family 7 member A1	ALDH7A1	Q9DBF1[f]	↑ 1.21	2	2	6
2. Protein synthesis, modification, and secretion								
Up-regulated								
4–7	2231	*N*-Ethylmaleimide-sensitive factor attachment protein, α	NAPA	P54921	↑ 1.48	6	6	29
4. Processing of peptides and neurotransmitters								
Up-regulated								
4–7	2683	Catechol *O*-methyltransferase	COMT	P22734	↑ 1.32	3	3	16
		Catechol *O*-methyltransferase (soluble)		P22734-2 (100%)				17
5. Cell adhesion, cytoskeleton, and related genes								
Up-regulated								
4–7	803	Cytoplasmic dynein 1 intermediate chain 2	DYNC1I2	Q62871	↑ 1.81	3	3	6.3
		Cytoplasmic dynein 1 intermediate chain 2 isoform 2B		Q62871-2 (99.1%)				6.3
		Cytoplasmic dynein 1 intermediate chain 2 isoform 2C		Q62871-3 (95.9%)				6.5
		DNCIC2 protein	DNCIC2	Q6AZ35 (98.6%)				6.3
4–7	1074	WD repeat protein 1	WDR1	Q5RKI0	↑ 1.35	12	12	31
4–7	1254	Chaperonin subunit θ	CCT8	XP_213673	↑ 1.24	10	10	16
		Chaperonin subunit θ		XP_001067000 (100%)				16
4–7	1634	Ezrin-radixin-moesin-binding phosphoprotein 50	SLC9A3R1	Q9JJ19	↑ 3.06	3	3	13
6. RNA synthesis/turnover								
Up-regulated								
4–7	2013	Nucleophosmin	NPM1	P13084	↑ 1.21	4	4	16
Down-regulated								
4–7	2778	Splicing factor, arginine/serine-rich 3	SFRS3	P84104	↓ 1.47	2	1	14
		Hypothetical protein		Q0ZFS8 (100%)				14
7. Cell cycle and related genes								
Up-regulated								
4–7	1667	NSFL1 cofactor p47, XY40 protein	NSFL1C	O35987	↑ 1.17	11	11	42
9. Apoptosis/endoplasmic reticulum stress-related								
Up-regulated								
6–9	1037	Annexin 11	ANXA11	Q5XI77	↑ 1.47	4	3	11
4–7	1233	Inositol 1,4,5-trisphosphate receptor type 2	ITPR2	P29995	↑ 1.88	2	1	1

[a] Abbreviated protein name according to iHOP and Swiss-Prot.
[b] The Swiss-Prot accession number (if no Swiss-Prot accession number was available, the NCBI accession number was used). If two different accession numbers were found with 100% identity, both are reported, the first one consistently the one with the best description. If an isoform or individual protein of a protein member could not be ruled out, different accession numbers are given, including the percent homology with the first one.
[c] -Fold regulation as calculated with the DeCyder 6.5 software ($p \leq 0.01$).
[d] Number of peptides sequenced by MS/MS.
[e] Number of unique sequences (in terms of amino acid sequence) when individually aligned using BLAST.
[f] Mouse accession number. For full information, please see Supplemental Table 1.

Downloaded from www.mcponline.org by on January 2, 2008

TABLE II

Identification of proteins with an altered protein expression level upon 24 h of IL-1β and IFN-γ incubation in INS-1E cells

pH	Spot no.	Full protein name	Protein name[a]	Swiss-Prot accession no.[b]	-Fold regulation[c]	No. peptides sequenced[d]	No. of unique peptides[e]	Sequence coverage
								%
1. Metabolism								
Up-regulated								
6–9	498, 529, 530, 533	Aconitate hydratase, aconitase	ACO2	Q9ER34	↑1.59, ↑1.31, ↑1.44, ↑1.16	9, 3, 4, 11	9, 3, 4, 11	16, 5, 8, 19
4–7	882	Glycerol-3-phosphate dehydrogenase	GPD2	P35571	↑1.38	4	4	8.4
6–9	985, 1009	Glutamate dehydrogenase 1	GLUD1	P10860	↑1.51, ↑1.27	2,3	2,3	6, 9
6–9	995	Leucine aminopeptidase 3	LAP3	Q68FS4	↑1.25	7	7	15
		Leucine aminopeptidase 3 isoform 2		Q68FS4-2 (100%)				16
6–9	1009	Glutaminase	GLS	P13264	↑1.27	3	3	7
		Glutaminase		Q8R421 (100%)				16
6–9	1037	Nicotinamide phosphoribosyltransferase	NAMPT	Q80Z29	↑1.47	6	6	16
		Nicotinamide phosphoribosyltransferase		Q2VT47 (100%)				16
6–9	1190, 1195	Similar to $NADP^+$-specific isocitrate dehydrogenase	IDH2	P56574	↑1.29, ↑1.21	10, 8	8, 6	25, 18
6–9	1286	Citrate synthase	CS	Q8VHF5	↑1.51	7	1	16
6–9	1286	Phosphoglycerate kinase 1	PGK1	P16617	↑1.51	2	1	10
6–9	1308	Creatine kinase	CKMT1	Q5BJT9	↑1.60	2	1	9
6–9	1463	Glyceraldehyde-3-phosphate dehydrogenase	GAPDH	P04797	↑2.04	4	0	15
6–9	1484	Transaldolase	TALDO1	Q9EQS0	↑1.56	1	1	4
6–9	1627	Fumarylacetoacetate hydrolase domain-containing 2A	FAHD2A	XP_215851	↑1.34	5	5	18
Down-regulated								
6–9	550	Aconitate hydratase, aconitase	ACO2	Q9ER34	↓2.31	9	9	15
4–7	814, 815, 816	NADH dehydrogenase (ubiquinone) Fe-S protein 1	NDUFS1	Q66HF1	↓1.44, ↓1.87, ↓2.23	4, 2, 3	4, 2, 3	6, 3, 7
6–9	953	Pyruvate kinase isozymes M2	PKM2	P11980-2	↓1.24	9	0	24
6–9	1030	Inosine 5′-monophosphate dehydrogenase 2	IMPDH2	Q6P9U9	↓1.25	4	4	11
6–9	1207	Pyruvate dehydrogenase E1 α 1	PDHA1	Q4FZZ4	↓1.25	10	1	24
4–7	1262	Inosine 5′-monophosphate dehydrogenase 1	IMPDH1	XP_342651	↓1.58	7	7	14
6–9	1389	Arginase-1	ARG1	P07824	↓1.15	12	12	40
4–7	1414	α -Enolase	ENO1	P04764	↓1.99	7	6	16
		α -Enolase		Q5EB49 (99.5%)				16
		α -Enolase		Q5BJ93 (100%)				16
6–9	1415	Acetyl-coenzyme A acetyltransferase 2	ACAT2	Q5XI22	↓1.77	6	6	26
		Ab2-076		Q7TP61 (100%)				26
6–9	1731	Fumarylacetoacetate hydrolase domain-containing 2A	FAHD2A	XP_215851	↓1.32	7	7	24
6–9	1750	Carbonyl reductase (NADPH) 1	CBR1	P47727	↓1.38	5	1	17
6–9	1899	Triose-phosphate isomerase 1	TPI1	P48500	↓1.28	5	1	30

Downloaded from www.mcponline.org by on January 2, 2008

TABLE II—*continued*

pH	Spot no.	Full protein name	Protein name[a]	Swiss-Prot accession no.[b]	-Fold regulation[c]	No. peptides sequenced[d]	No. of unique peptides[e]	Sequence coverage
								%
4–7	1962	Ester hydrolase C11orf54 homolog	C11ORF54	Q5U2Q3	↓1.37	2	2	8
6–9	2155	Nucleoside-diphosphate kinase B	NME2	P19804	↓1.21	9	5	54
4–7	2187	Glyoxalase domain-containing protein 4	GLOD4	Q5I0D1	↓1.37	6	6	23.2
2. Protein synthesis, modification, and secretion								
Up-regulated								
4–7	242	150-kDa oxygen-regulated protein	HYOU1	Q63617	↑1.51	7	7	9
		Hyou1 protein		Q6P136 (99.4%)				9
6–9	958, 985	Elongation factor 2	EEF2	P05197	↑1.75, ↑1.51	8, 4	3, 0	12, 7
4–7	1013	GRP 75 kDa	HSPA9	P48721	↑1.30	4	3	8
4–7	1504	Dolichyl-diphosphooligosaccharide-protein glycotransferase	DDOST	Q641Y0	↑1.64	2	2	5.8
4–7	2332	Proteasome activator complex subunit 2	Q63798	PSME2	↑1.44	7	6	25.3
4–7	2962, 2963	GRP78; BiP	HSPA5	P06761	↑2.69, ↑3.52	9, 14	9, 14	19, 24
Down-regulated								
4–7	902	GRP78; BiP	HSPA5	P06761	↓2.68	11	11	27
4–7	922, 931, 971	Heat shock 70-kDa protein 8	HSPA8	P63018	↓1.46, ↓1.47, ↓1.54	7, 11, 3	2, 5, 1	16, 21, 7
4–7	994	GRP 75 kDa	HSPA9	P48721	↓1.91	5	4	10
4–7	1062	Serine/threonine-protein kinase PAK 2	PAK2	Q64303	↓1.20	4	2	11
4–7	1463	26 S protease regulatory subunit 6B	PRS6B	Q63570	↓1.33	6	6	18
4–7	1760	Ubiquitin-conjugating enzyme E2Z	UBE2Z	Q3B7D1	↓1.70	9	9	29
4–7	2140	*N*-Ethylmaleimide-sensitive factor attachment protein, α	NAPA	P54921	↓1.48	6	6	29
3. Ionic channels, ion transporters, and related								
Up-regulated								
6–9	1095	H^+-transporting two-sector ATPase	ATP5A1	P15999	↑1.47	12	12	31
6–9	1618	Voltage-dependent anion-selective channel protein 1	VDAC1	Q9Z2L0	↑1.30	9	9	52
		Voltage-dependent anion channel 1		A1L125 (100%)				52
4–7	2386	Chloride intracellular channel protein 4	CLIC4	Q9Z0W7	↑1.52	5	4	32.5
		Mitochondrial chloride intracellular channel 4		A3FM27 (98.4%)				32.5
Down-regulated								
4–7	809	Sodium channel protein type 9 α subunit	SCN9A	O08562	↓1.95	3	3	1.6
6–9	1951	Voltage-dependent anion-selective channel protein 1	VDAC1	Q9Z2L0	↓2.15	6	6	36
		Voltage-dependent anion channel 1		A1L125 (100%)				36
4. Processing of peptides and neurotransmitters								

Downloaded from www.mcponline.org by on January 2, 2008

TABLE II—*continued*

pH	Spot no.	Full protein name	Protein name[a]	Swiss-Prot accession no.[b]	-Fold regulation[c]	No. peptides sequenced[d]	No. of unique peptides[e]	Sequence coverage
								%
Down-regulated								
4–7	979, 994	Neuroendocrine convertase 1	PCSK1	P28840	↓1.71, ↓1.91	2, 4	2, 4	6, 7
4–7	1003, 1007, 1024, 1060, 1084, 1090	Neuroendocrine convertase 2	PCSK2	P28841	↓3.81, ↓5.70, ↓2.81, ↓1.48, ↓1.69, ↓2.24	2, 2, 3, 9, 2, 2	2, 2, 3, 9, 2, 2	4, 4, 6, 15, 4, 4
5. Cell adhesion, cytoskeleton, and related genes								
Up-regulated								
4–7	1505	Ezrin-radixin-moesin-binding phosphoprotein 50	SLC9A3R1	Q9JJ19	↑3.55	3	3	13
4–7	1659	Actin β	ACTB	P60711	↑1.50	6	0	16
		Actin γ	ACTG1	P63259 (98.9%)				16
4–7	1665	Actin β	ACTB	P60711	↑1.63	4	1	13.1
		Actin γ	ACTG1	P63259 (98.9%)				13.1
		Actin, γ -enteric smooth muscle	ACTG2	P63269 (93.6%)				13
		Actin, α skeletal muscle	ACTA1	P68136 (93.6%)				13
		Actin, α cardiac muscle 1	ACTC1	P68035 (94.1%)				13
		Actin, aortic smooth muscle	ACTA2	P62738 (94.1%)				13
		Actin α cardiac 1	ACTC1	A0JPJ4 (94.1%)				13
4–7	1668	Actin β	ACTB	P60711	↑1.70	4	0	15
		Actin γ	ACTG1	P63259 (98.9%)				15
4–7	2723	Cofilin-1	CFL1	P45592	↑2.25	6	6	44
Down-regulated								
6–9	670	Septin 9	SEPT9	Q9QZR6	↓1.50	2	1	5
4–7	741	Mitofilin	IMMT	Q3KR86	↓1.33	7	7	16
4–7	753	Glial fibrillary acidic protein	GFAP	P47819	↓1.49	2	1	6
		Glial fibrillary acidic protein ϵ (fragment)		A1E252 (100%)				16
		Glial fibrillary acidic protein, isoform 2		P47819-2 (100%)				6
4–7	814, 816	Lamin-B2	LMNB2	P21619[f]	↓1.44, ↓2.23	4, 5	2, 5	7, 8
6–9	816	Chaperonin subunit 6a, ζ	CCT6A	Q3MHS9	↓1.74	5	2	11
4–7	1049	α -Internexin	INA	P23565	↓1.46	7	7	19
4–7	1117	Chaperonin subunit θ	CCT8	XP_213673	↓1.46	10	10	16
		Chaperonin subunit θ		XP_001067000 (100%)				16
4–7	1317	Group-specific component	GC	Q68FY4	↓2.07	2	2	6
		Vitamin D-binding protein		P04276 (99.8%)				6
4–7	2214	Group-specific component	GC	Q68FY4	↓1.94	5	1	17
6. RNA synthesis/ turnover								

Downloaded from www.mcponline.org by on January 2, 2008

TABLE II—*continued*

pH	Spot no.	Full protein name	Protein name[a]	Swiss-Prot accession no.[b]	-Fold regulation[c]	No. peptides sequenced[d]	No. of unique peptides[e]	Sequence coverage
								%
Up-regulated								
6–9	529, 530	ATP-dependent RNA helicase DDX1	DDX1	Q641Y8	↑1.31, ↑1.44	6, 11	5, 10	9, 15
6–9	590	ATP-dependent RNA helicase DDX3X	DDX3X	XP_228701	↑4.95	13	11	21
4–7	1122	Tyrosyl-tRNA synthetase	YARS	Q4KM49	↑1.44	3	3	7
Down-regulated								
4–7	706	Eukaryotic translation initiation factor 4B	EIF4B	Q5RKG9	↓1.62	3	3	7
4–7	1049, 1056, 1075, 1174, 1211, 1216	Heterogeneous nuclear ribonucleoprotein K	HNRPK	P61980	↓1.46, ↓1.92, ↓3.02, ↓1.25, ↓1.59, ↓2.96	3, 9, 2, 7, 6, 6	3, 9, 2, 7, 6, 6	7, 25, 5, 23, 20, 16
		Hnrpk protein		Q5D059 (99.8%)				7, 25, 5, 23, 20, 16
4–7	1262	Heterogeneous nuclear ribonucleoprotein H1	HNRPH1	Q8VHV7	↓1.58	4	1	19
		Heterogeneous nuclear ribonucleoprotein H′		Q6AY09 (96%)				15
		Hnrph1 protein		A1L1J1 (93.8%)				16
4–7	1279	Heterogeneous nuclear ribonucleoprotein H1	HNRPH1	Q8VHV7	↓1.72	4	0	17.8
7. Cell cycle and related genes								
Down-regulated								
4–7	1546	N-Myc downstream regulated 1	NDRG1	Q6JE36	↓1.48	6	6	12
4–7	1571	NSFL1 cofactor p47, XY40 protein	NSFL1C	O35987	↓1.28	11	11	42
4–7	2074	Proliferating cell nuclear antigen, Cyclin	PCNA	P04961	↓2.07	6	6	28
8. Defense/repair								
Up-regulated								
6–9	1994	Mn-superoxide dismutase, mitochondrial	SOD2	P07895	↑2.50	5	5	40
6–9	2014	Peroxiredoxin-1, thioredoxin peroxidase 2	PRDX1	Q63716	↑7.57	2	2	11
Down-regulated								
4–7	1463	Protein-disulfide isomerase A6/P5; thioredoxin d-c prot7	PDIA6	Q63081	↓1.33	8	8	31
4–7	1996	Thioredoxin-like protein 1	TXNL1	Q920J4	↓1.46	6	6	36
6–9	1975	Peroxiredoxin-1, thioredoxin peroxidase 2	PRDX1	Q63716	↓2.67	8	8	47
4–7	2613	Peroxiredoxin III	PRDX3	Q9Z0V6	↓1.29	1	1	5
9. Apoptosis/ endoplasmic reticulum stress-related								
Up-regulated								
6–9	1037	Annexin 11	ANXA11	Q5XI77	↑1.47	4	3	11
4–7	1097	Inositol 1,4,5-trisphosphate receptor type 2	ITPR2	P29995	↑2.19	2	1	1

Downloaded from www.mcponline.org by on January 2, 2008

TABLE II—*continued*

pH	Spot no.	Full protein name	Protein name[a]	Swiss-Prot accession no.[b]	-Fold regulation[c]	No. peptides sequenced[d]	No. of unique peptides[e]	Sequence coverage
								%
10. Miscellaneous								
Up-regulated								
4–7	905	Serum albumin	ALB	P02770	↑ 1.67	1	1	2.4
4–7	925	Neogenin	NEO1	P97603	↑ 1.22	2	2	2
4–7	533	Major vault protein	MVP	Q62667	↑ 1.54	11	11	19.3
Down-regulated								
6–9	1908	Similar to stromal cell-derived factor 2 precursor	SDF2	XP_213377	↓ 1.16	3	3	31.6

[a] Abbreviated protein name according to iHOP and Swiss-Prot.

[b] The Swiss-Prot accession number (if no Swiss-Prot accession number was available, the NCBI accession number was used). If two different accession numbers were found with 100% identity, both are reported, the first one consistently the one with the best description. If an isoform or individual protein of a protein member could not be ruled out, different accession numbers are given, including the percent homology with the first one.

[c] -Fold regulation as calculated with the DeCyder 6.5 software ($p \leq 0.01$).

[d] Number of peptides sequenced by MS/MS.

[e] Number of unique sequences (in terms of amino acid sequence) when individually aligned using BLAST.

[f] Mouse accession number. For full information, please see Supplemental Table 1.

DISCUSSION

In the present study we have identified 129 protein spots with an altered abundance or PTM by IL-1β, IFN-γ, or IFN-γ + IL-1β treatment of INS-1E cells, a rat insulin-producing cell line used as a model for β-cell dysfunction and death in type 1 diabetes. By applying the 2D DIGE technique to investigate the differential protein expression profiles we identified relevant proteins with a high confidence rate not possible by classical 2DE. The importance of the differentially expressed proteins was further supported by the close linkage they appear to have in the predicted interaction network. Indeed this suggests that the proteins identified, although belonging to a broad range of different classes and functional pathways, interact with each other in close relationships, creating a functional network that may regulate β-cell dysfunction and eventually β-cell death.

The concentrations of cytokines used in the present study clearly act synergistically in inducing apoptotic cell death in INS-1E cells. Indeed only minor alterations in the proportion of apoptotic cells were observed upon exposure to either IL-1β or IFN-γ alone, whereas the combined cytokines resulted in a dramatic increase in apoptosis. This is reflected in the observed changes in protein profiles where again a synergistic effect between IL-1β and IFN-γ was observed with major changes in protein levels only occurring in the combined treatment and this after a long incubation of 24 h.

Because the primary goal of β-cells is to process and secrete high amounts of insulin, it is not surprising that different proteins playing a crucial role in insulin biosynthesis were altered in expression following cytokine treatment (Fig. 2). In accordance with the reported increase in the proinsulin/insulin ratio and a decreased insulin secretion upon cytokine treatment (4, 6, 34), a clear down-regulation of the different isoforms of PCSK1 and PCSK2, the enzymes responsible for conversion of proinsulin to insulin, was observed. Another interesting protein important in the processing of insulin is thioredoxin-like protein 1 (TXNL1). TXNL1 reduces the disulfide bridges of insulin, thereby initiating the degradation of insulin (35). The observed down-regulation of this protein is yet another detrimental effect of IL-1β and IFN-γ on the insulin processing capacities in INS-1E cells.

In recent years, it has become clear that ER stress is implicated in β-cell death (3). One of the well known effects of cytokines on INS-1E cells is the formation of NO (2). Although inducible nitric-oxide synthase itself could not be detected in the 2D gels because of the high molecular weight of this protein, we observed two abundantly expressed ER chaperones, BiP/GRP78 and ORP150, that were clearly shifted toward more acidic forms suggestive for phosphorylation or ribosylation of these proteins. Although there are many studies implicating an important role of ER chaperones in β-cell death, very little information is available on the functional impact of their phosphorylation or ribosylation status. Over-

Downloaded from www.mcponline.org by on January 2, 2008

TABLE III

Identification of proteins with an altered protein expression level upon 24 h of IL-1β incubation in INS-1E cells

pH	Spot no.	Full protein name	Protein name[a]	Swiss-Prot accession no.[b]	-Fold regulation[c]	No. peptides sequenced[d]	No. of unique peptides[e]	Sequence coverage
								%
1. Metabolism								
Up-regulated								
6–9	304	Aconitate hydratase, aconitase	ACO2	Q9ER34	↑1.44	9	9	13.4
6–9	846	Serine hydroxymethyltransferase	SHMT2	Q5U3Z7	↑1.26	7	7	17.1
6–9	1308	Creatine kinase	CKMT1	P25809	↑3.08	9	6	21.1
6–9	1471	Electron transfer flavoprotein subunit α	ETFA	P13803	↑1.36	3	3	16.9
4–7	1538	Succinate-coenzyme A ligase	SUC1G2	Q68FT4	↑1.15	7	7	23.6
		Succinate-coenzyme A ligase (fragment of Q68FT4)		Q5EBA9 (100%)				26.4
		Succinate-coenzyme A ligase (fragment of Q68FT4)		Q499V7 (100%)				23.8
Down-regulated								
6–9	305	Aconitate hydratase, aconitase	ACO2	Q9ER34	↓1.51	12	12	21.1
4–7	666	Glycerol-3-phosphate dehydrogenase	GPD2	P35571	↓1.61	6	6	10.1
4–7	815	NADH-ubiquinone oxidoreductase 75-kDa subunit	NDUFS1	Q66HF1	↓1.38	12	12	23.4
6–9	898	NADH dehydrogenase (Ubiquinone) flavoprotein 1	NDUFV1	Q5XIH3	↓1.49	9	9	25.4
4–7	1414	α -Enolase	ENO1	P04764	↓1.87	5	4	15.7
		α -Enolase		Q5BJ93 (100%)				15.7
		α -Enolase		Q5EB49 (99.5%)				15.7
2. Protein synthesis, modification, and secretion								
Up-regulated								
4–7	735	75-kDa glucose-regulated protein, GRP75	HSPA9	P48721	↑1.20	11	10	18.5
4–7	962	Syntaxin-binding protein 1-like 2	STXBP1L2	Q62991	↑1.19	5	5	14.4
3. Ionic channels, ion transporters, and related								
Up-regulated								
4–7	1150	Vacuolar ATP synthase subunit B, brain isoform	VATB2	P62815	↑1.11	7	7	19.8
4–7	2386	Chloride intracellular channel protein 4	CLIC4	Q9Z0W7	↑1.39	5	4	32.5
				A3FM27 (98.4%)				32.5
4. Processing of peptides and neurotransmitters								
Down-regulated								
4–7	1024,1084, 1090	Neuroendocrine convertase 2	PCSK2	P28841	↓1.55, ↓1.44, ↓1.63	5, 6, 5	5, 6, 5	13, 13, 10
5. Cell adhesion, cytoskeleton, and related genes								

Downloaded from www.mcponline.org by on January 2, 2008

TABLE III—*continued*

pH	Spot no.	Full protein name	Protein name[a]	Swiss-Prot accession no.[b]	-Fold regulation[c]	No. peptides sequenced[d]	No. of unique peptides[e]	Sequence coverage
								%
Up-regulated								
4–7	1510	Actin β	ACTB	P60711	↑1.28	5	0	17.6
		Actin γ	ACTG1	P63259 (98.9%)				17.6
Down-regulated								
4–7	803	Cytoplasmic dynein 1 intermediate chain 2	DYNC1I2	Q62871	↓1.12	3	3	6.3
		Cytoplasmic dynein 1 intermediate chain 2 isoform 2B		Q62871–2 (99.1%)				6.3
		Cytoplasmic dynein 1 intermediate chain 2 isoform 2C		Q62871–3 (95.9%)				6.5
		DNCIC2 protein	DNCIC2	Q6AZ35 (98.6% identity)				6.3
4–7	2214	Vitamin D-binding protein	GC	P04276	↓1.35	4	4	14.1
		Group-specific component		Q68FY4 (99.8%)				14.1
6. RNA synthesis/turnover								
Up-regulated								
4–7	545	Eukaryotic translation initiation factor 4B	EIF4B	Q5RKG9	↑1.35	4	4	8
Down-regulated								
4–7	1075	Heterogeneous nuclear ribonucleoprotein K	HNRPK	P61980	↓1.81	5	5	13.6
		Hnrpk protein		Q5D059 (99.8%)				13.6
8. Defense/repair								
Up-regulated								
4–7	780	Similar to guanylate nucleotide-binding protein 4	GBP4	XP_227762	↑1.67	6	6	9.2
4–7	1305	Protein-disulfide isomerase A6	PDIA6	Q63081	↑1.20	4	4	14
4–7	1379	Interferon-inducible GTPase	IFI47	Q6NYB8	↑2.08	7	4	22.2
6–9	1994	Mn-superoxide dismutase, mitochondrial	SOD2	P07895	↑3.01	4	4	25.3
4–7	2131	Proteasome activator complex subunit 1	PSME1	Q63797	↑1.40	6	1	27.7
4–7	2332	Proteasome activator complex subunit 2	PSME2	Q63798	↑1.54	7	6	25.3
10. Miscellaneous								
Up-regulated								
4–7	321, 533	Major vault protein	MVP	Q62667	↑1.51, ↑2.01	11, 11	11, 11	14.7, 19.3

[a] Abbreviated protein name according to iHOP and Swiss-Prot.

[b] The Swiss-Prot accession number (if no Swiss-Prot accession number was available, the NCBI accession number was used). If two different accession numbers were found with 100% identity, both are reported, the first one consistently the one with the best description. If an isoform or individual protein of a protein member could not be ruled out, different accession numbers are given, including the percent homology with the first one.

[c] -Fold regulation as calculated with the DeCyder 6.5 software ($p \leq 0.01$).

[d] Number of peptides sequenced by MS/MS.

[e] Number of unique sequences (in terms of amino acid sequence) when individually aligned using BLAST. For full information, please see Supplemental Table 1.

Downloaded from www.mcponline.org by on January 2, 2008

TABLE IV

Identification of proteins with an altered protein expression level upon 24 h of IFN-γ incubation in INS-1E cells

pH	Spot no.	Full protein name	Protein name[a]	Swiss-Prot accession no.[b]	-Fold regulation[c]	No. peptides sequenced[d]	No. of unique peptides[e]	Sequence coverage
								%
1. Metabolism								
Up-regulated								
4–7	991	Glucose-6-phosphate 1-dehydrogenase	G6PD	P05370	↑1.43	10	10	23.9
Down-regulated								
4–7	1005	Pyruvate kinase isozymes R/L	PKLR	P12928	↓1.34	6	6	12.4
		Pyruvate kinase isozyme L	PKL	P12928–2 (100%)				13.1
2. Protein synthesis, modification, and secretion								
Up-regulated								
4–7	1156	Tryptophanyl-tRNA synthetase, cytoplasmic	WARS	Q6P7B0	↑1.96	6	6	17.5
4–7	1504	Dolichyl-diphosphooligosaccharide-protein glycotransferase	DDOST	Q641Y0	↑1.89	2	2	5.8
5. Cell adhesion, cytoskeleton, and related genes								
Up-regulated								
4–7	1510	Actin β	ACTB	P60711	↑1.53	5	0	17.6
		Actin γ	ACTG1	P63259 (98.9%)				17.6
Down-regulated								
4–7	2214	Vitamin D-binding protein	GC	P04276	↓1.27	4	4	14.1
		Group-specific component		Q68FY4 (99.8%)				14.1
6. RNA synthesis/turnover								
		Down-regulated						
4–7	1075	Heterogeneous nuclear ribonucleoprotein K	HNRPK	P61980	↓1.30	5	5	13.6
8. Defense/repair								
Up-regulated								
4–7	599, 631	Interferon-induced GTP-binding protein Mx2	MX2	P18589	↑1.93, ↑3.12	6, 9	3, 6	14.4, 18.4
		Interferon-induced GTP-binding protein Mx3	MX3	P18590 (98.8%)				
		Myxovirus (influenza virus) resistance 2	MX2	Q499Q3 (99.2%)				
4–7	780	Similar to guanylate nucleotide-binding protein 4	GBP4	XP_227762	↑3.70	6	6	9.2
4–7	1379	Interferon-inducible GTPase	IFI47	Q6NYB8	↑9.32	7	4	22.2
4–7	1390	Interferon-γ -induced GTPase, Ac2–233	IGTP	Q7TPJ1	↑9.82	7	4	6.1
4–7	2131	Proteasome activator complex subunit 1	PSME1	Q63797	↑2.10	6	1	27.7
4–7	2332	Proteasome activator complex subunit 2	PSME2	Q63798	↑2.01	7	6	25.3
9. Apoptosis/endoplasmic reticulum stress-related								
Up-regulated								
4–7	1097	Inositol 1,4,5-trisphosphate receptor type 2	ITPR2	P29995	↑2.92	2	1	0.9
10. Miscellaneous								
Up-regulated								
4–7	321, 533	Major vault protein	MVP	Q62667	↑1.57, ↑1.67	11, 11	11, 11	14.7, 19.3

[a] Abbreviated protein name according to iHOP and Swiss-Prot.
[b] The Swiss-Prot accession number (if no Swiss-Prot accession number was available, the NCBI accession number was used). If two different accession numbers were found with 100% identity, both are reported, the first one consistently the one with the best description. If an isoform or individual protein of a protein member could not be ruled out, different accession numbers are given, including the percent homology with the first one.
[c] -Fold regulation as calculated with the DeCyder 6.5 software ($p \leq 0.01$).
[d] Number of peptides sequenced by MS/MS.
[e] Number of unique sequences (in terms of amino acid sequence) when individually aligned using BLAST. For full information, please see Supplemental Table 1.

Downloaded from www.mcponline.org by on January 2, 2008

TABLE V
Protein identifications based on single peptide sequences

Spot no.	Full protein name	Protein name	Swiss-Prot accession no.	Ion score	No. peptides sequenced	Sequence coverage	Precursor *m/z*	Charge	Score	Expect	Sequences of MS/MS
						%					
1484	Transaldolase	TALDO1	Q9EQS0	47	1	4	1392.5619	+1	47	0.0011	ALAGCDFLTISPK
2613	Peroxiredoxin III	PRDX3	Q9Z0V6	101	1	5	1476.8174	+1	101	1.00e−08	DYGVLLESAGIALR
905	Serum albumin	ALB	P02770	75	1	2.4	1749.5309	+1	75	2.10e−07	ECCHGDLLECADDR

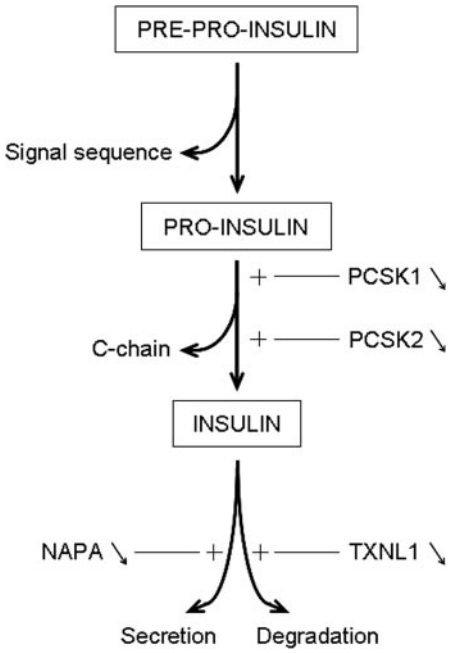


FIG. 2. **Scheme of insulin formation.** The proteins involved that are differentially expressed after IFN-γ and IL-1β treatment are displayed. See "Discussion" for details. For full names of abbreviations, see Tables I–IV.

expression of BiP/GRP78 has a protective effect on β-cell death (36), and the present observations on decreased BiP expression is in agreement with our previous findings on an IFN-γ-induced decrease in BiP mRNA expression (37, 38). Furthermore phosphorylation of BiP results in a lower binding capacity for proteins (39, 40) that, together with the above described decrease in expression of non-phosphorylated BiP, may aggravate ER stress by interfering with the clearance of unfolded or misfolded proteins (41).

ORP150, another ER chaperone, also shifted toward expression of more acidic isoforms although less markedly than for BiP/GRP78. Increased ORP150 expression improves insulin resistance in animal models of type 2 diabetes and may have a protective role against β-cell death (42). In this context, it will be of interest to study the functional impact of the observed ORP150 PTM.

Another chaperone modified by cytokine treatment is HSPA8, which mainly resides in the cytosol. HSPA8 is an ATP-dependent chaperone (43) and has antiapoptotic effects (44). The observed down-regulation of this chaperone in all three different isoforms identified may hamper β-cell defenses. Opposite results have been described in neonatal rat islets where an increase in HSPA8 protein expression was observed upon treatment with IL-1β alone (45). Because in our experiments INS-1E cells were exposed to IL-1β + IFN-γ, this points toward an aggravating effect of IFN-γ on β-cell death via inhibition of molecular chaperones as shown previously in both INS-1E and primary β-cells (38). The fourth cytokine-modified member of the hsp70 family is HSPA9, a mitochondrial chaperone involved in protein folding and intracellular trafficking (46). HSPA9 has been implicated in the regulation of apoptosis through transcriptional inactivation of the tumor suppressor protein p53 (47).

Apart from NO formation, another detrimental effect of cytokine exposure to β-cells is the formation of reactive oxygen species (ROS). The observed induction of SOD2 points toward a protective response of the INS-1E cells against cytokine-induced ROS formation in agreement with published findings from microarray (9) or Western blot (10) analyses. However, a longer exposure of β-cells to cytokines will finally result in down-regulation of SOD2, further aggravating β-cell death (10). SOD2-mediated conversion of superoxide molecules will result in a high local production of H_2O_2. This hydrogen peroxide will be eliminated by reduction to H_2O by another group of proteins, the peroxiredoxins (48), and we have presently observed an up-regulation of the cytoplasmic PRDX1. It is puzzling why the other isoform of PRDX1 was down-regulated, which was also the case for the mitochondrial PRDX3, which exerts a function similar to that of PRDX1 (49). PRDX1 and PRDX3 use thioredoxins as electron donors to reduce hydrogen peroxide, and two proteins containing thioredoxin domains were presently identified: the ER protein-disulfide isomerase A6/P5 (PDIA6) and the cytoplasmic TXNL1. Cytokines down-regulated both these proteins, which may impair the β-cell ROS scavenging machinery. As a whole, these observations suggest a complex regulation of the SOD2-peroxiredoxin-thioredoxin system by cytokines that may initially contribute to free radical scavenging but, in the case of protracted exposure to cytokines, may contribute to cell death (10).

Different members of two large groups of proteins playing crucial roles in RNA metabolism were identified in the present study, namely the hnRNPs and the DEAD box family proteins.

Downloaded from www.mcponline.org by on January 2, 2008

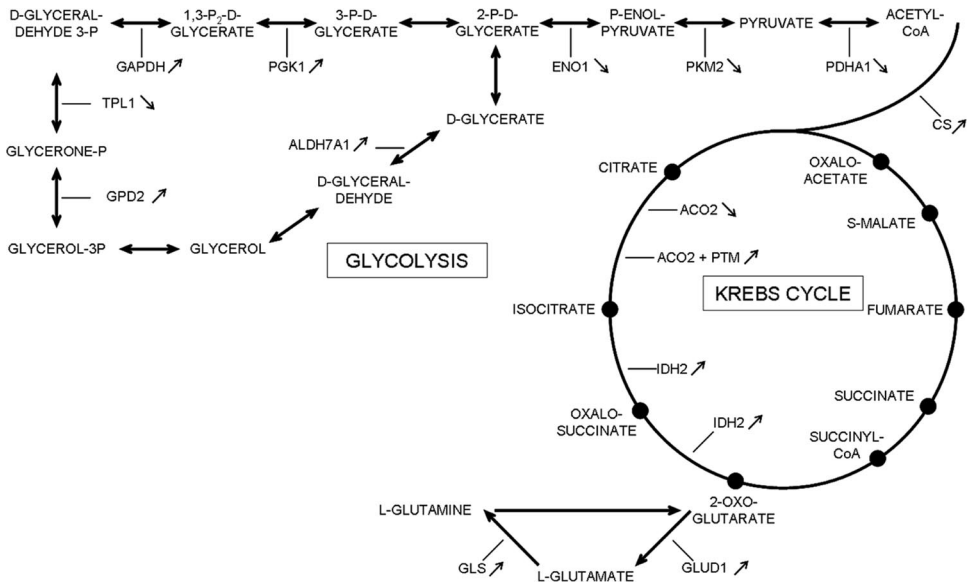


FIG. 3. **Scheme of metabolic pathway.** The proteins involved that are differentially expressed after IFN-γ and IL-1β treatment are displayed. Many proteins involved in the glycolytic as well as in the Krebs cycle (as indicated) are altered in expression. For full names of abbreviations, see Tables I–IV.

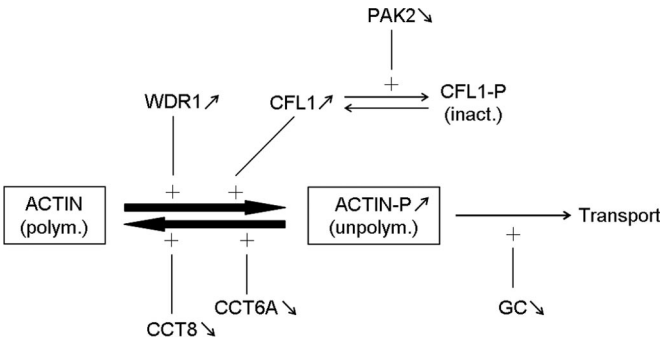


FIG. 4. **Scheme of actin formation.** The proteins involved that are differentially expressed after IFN-γ and IL-1β treatment are displayed. Central is the increased phosphorylation of actin. WD repeat-containing protein 1 (*WDR1*) and cofilin (*CFL*) are involved in depolymerization of β-actin (29, 30). Serine/threonine-protein kinase (*PAK2*) is involved in phosphorylation of cofilin, resulting in its inactivation (*inact*.) (31). Chaperonin subunit θ (*CCT8*) and chaperonin subunit ζ (*CCT6A*), two chaperones of β-actin, are involved in molecular chaperoning, in the production and folding of native actin, and in elongation of actin filaments (32). Vitamin D-binding protein (*GC*) plays a role in the transport of depolymerized actin molecules (33). *-P* indicates phosphorylation. *polym.*, polymerized; *unpolym.*, unpolymerized.

The main functions of hnRNPs, a class of abundantly expressed proteins, are in transcription, processing of pre-mRNA, alternative splicing, and nucleocytoplasmic shuttling of proteins. hnRNPs themselves are prone to alternative splicing and PTM such as cleavage by caspases (50), altering their activation state. In turn, by having important functions in mRNA splicing (*e.g.* splicing of Bcl family members) and nucleocytoplasmic shuttling they play an important role in regulation of apoptosis (50). Especially hnRNP K (six spots, pH 4–7) seems to be prone to PTMs. The six different spots that have been identified can be divided into two distinct groups of modified isoforms. In addition, the location of the spots suggests a post-translational cleavage. Although this needs further investigation, cleavage by caspases, accompanied by subcellular translocation, may be involved in this process (50, 51). Two different members of the DEAD box protein family were also identified as altered by cytokine treatment, namely DDX1 and DDX3X. DEAD box proteins are implicated in diverse cellular processes such as RNA splicing, ribosome assembly, and translation initiation. Although the function of DDX1 and DDX3X is poorly understood, the increased expression of DDX3X correlates with its reported proapoptotic role in NIH-3T3 fibroblasts (52).

Compared with previous microarray data (7, 53, 54), few proteins, *e.g.* SOD2, PCSK1, PCSK2, and BiP/GRP78, were found to correlate with the present proteomics data. Microarray data of cytokine-treated rat or human β-cells (7, 9, 53, 55, 56) revealed many genes that were classified as playing a role in mononuclear cell infiltration/activation (*e.g.* chemokines), signal transduction (*e.g.* STAT1, IRF1, and c-*jun*), and dysfunction (*e.g.* insulin, pancreas/duodenum homeobox 1 (*pdx-1*) and insulin gene enhancer protein (*isl-1*)). Several of these genes were confirmed at the protein level by ELISA, Western blotting, or other methods (5, 57, 58). The majority of these proteins, however, were not detected in the present study. A weak point of 2DE in general is the limitation of protein separation for extreme molecular weight and pI, low abundance, or membrane proteins. This is probably the reason why we could not detect for instance inducible nitric-oxide synthase, chemokines, or transcription factors as modified by exposure to cytokines. It may be possible to overcome these problems, to a certain extent, by making use of narrower pH ranges or prefractionation techniques, but this

Downloaded from www.mcponline.org by on January 2, 2008

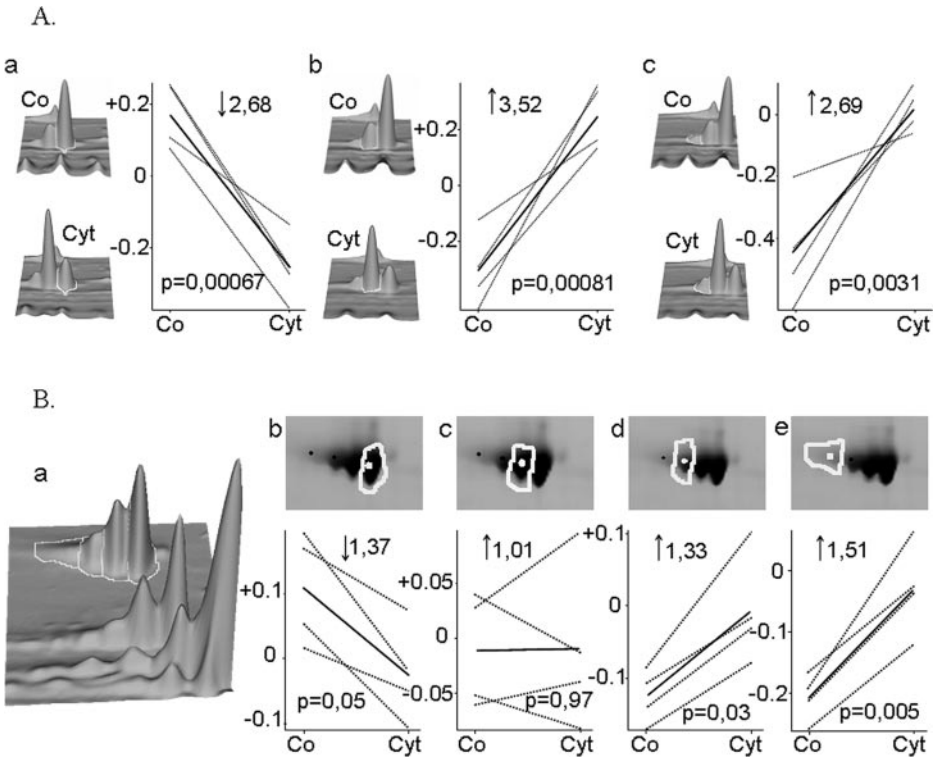


FIG. 5. *A*, regulation of BiP/GRP78 24 h after IL-1β/IFN-γ treatment. Each panel consists of two representative three-dimensional images, one of control (*Co*) and one of cytokine-treated (*Cyt*) samples, and the graph view of the DeCyder analysis ($n = 4$) for each particular spot with the standardized log abundance in the *y axis*. *a*, spot 902, the unmodified isoform of BiP/GRP78; *b* and *c*, spot 2963/2962, BiP/GRP78 undergoing PTM. *B*, regulation of ORP150 24 h after IL-1β/IFN-γ treatment. *a*, representative three-dimensional view of the "spot train." *b–e*, graph views of the DeCyder analysis ($n = 4$) for each particular spot with the standardized log abundance in the *y* axis. Spot 264 (*b*), the unmodified isoform of ORP150; spots 259 (*c*), 247 (*d*), and 242 (*e*), different forms of ORP150 undergoing PTM.

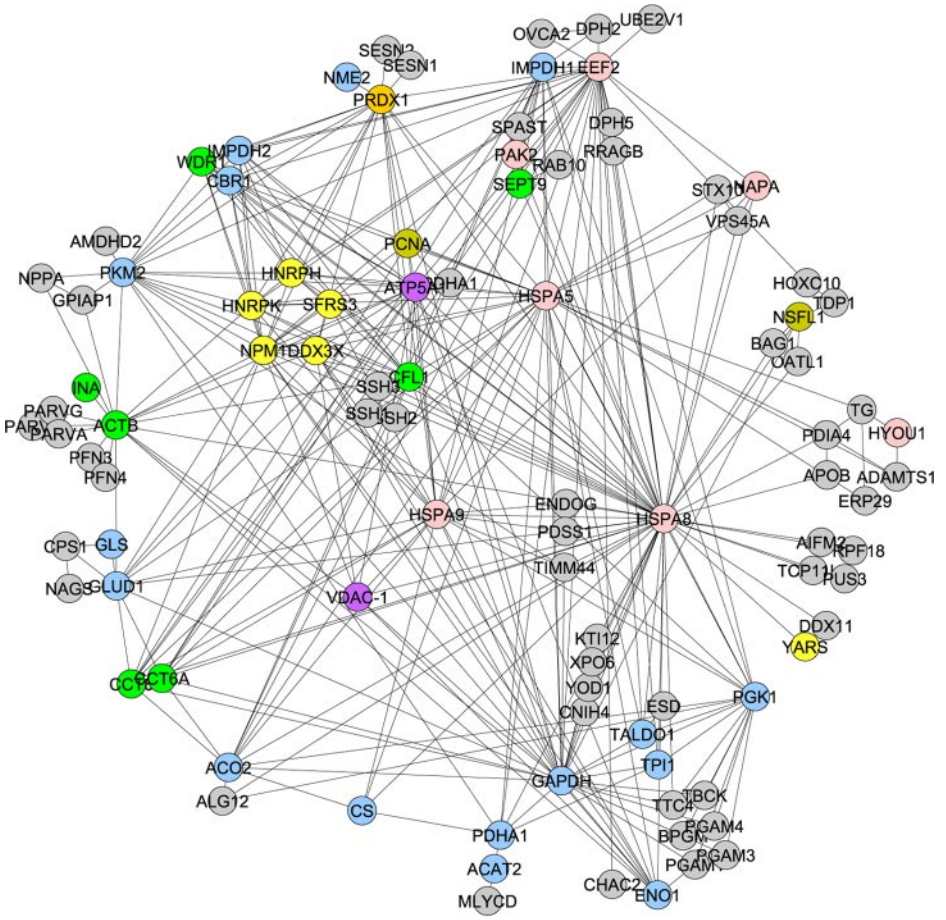


FIG. 6. **Protein interaction network revealing that 42 of the differentially expressed proteins identified constitute a significant interaction ($p < 1.27e-05$).** *Colored circles* represent proteins that were identified in this study, and *gray circles* represent interconnecting proteins revealed by the network software program. A maximum of two interconnecting proteins is allowed. The identified proteins were colored according to their function (as classified in Tables I–IV): proteins involved in metabolism, *blue*; cell adhesion and cytoskeleton, *green*; RNA synthesis/turnover, *yellow*; protein synthesis/modification, *pink*; ionic channels and related proteins, *purple*; cell cycle, *brown*; and defense/repair mechanisms, *orange*. Central in the network are the molecular chaperones HSPA5 (BiP/GRP78), HSPA8, and HSPA9 (*pink*) and the RNA synthesis/turnover proteins (*yellow*). For full names of abbreviations, see Tables I–IV.

Downloaded from www.mcponline.org by on January 2, 2008

demanding approach was beyond the scope of the present study. On the other hand we identified many new proteins, not previously identified by microarray analysis, that play a role in for instance metabolism, insulin biosynthesis, cytoskeleton organization, ER stress and defense/repair, and RNA metabolism. Many of these proteins are abundantly expressed and are undergoing PTMs, which could of course not be detected by microarray analysis. It is therefore beyond any doubt that the present data are to a great extent complementary to the previously performed microarray results and add new interesting insights into the mechanisms involved in cytokine-induced β-cell dysfunction and apoptotic cell death.

In addition, treatment with a combination of IL-1β and IFN-γ clearly has much more pronounced effects on the global protein profile, as discussed above, as compared with the single cytokine treatments. Of note, although only 17 proteins were identified as changed by IFN-γ alone, some of these changes are very pronounced and not observed in the combination-treated cells, such as interferon-inducible GTPase (9.32-fold induced), interferon-γ-induced GTPase (9.82-fold induced), or guanylate nucleotide-binding protein 4 (3.70-fold induced). Interestingly these proteins are involved in cellular defense mechanisms. This suggests that treatment with IFN-γ alone at the concentration used may activate different protective mechanisms resulting in an adaptation of the cells against the cytotoxic effect of IFN-γ consistent with the finding that no induction of apoptosis when using the single cytokine is observed. Next to this, also an interesting picture is observed for IL-1β alone. Here most proteins that are affected are involved in β-cell function and not β-cell death. This is in concordance with previous observations that IL-1β plays a crucial role in inhibiting β-cell function (4, 5), supported by the intriguing recent observations that blocking IL-1β in type 2 diabetic patients partially restores β-cell function (59). The role of IL-1β in *in vivo* β-cell survival and death, however, is still controversial. Conflicting reports are present in the literature on whether IL-1β actually induces apoptosis in levels that are of relevant impact to affect β-cell mass *in vivo* or whether, under some conditions, it actually promotes β-cell survival (60, 61). Issues in the different reports are timing of exposure, dose of IL-1β used, and the presence of other cytokines that may amplify or inhibit IL-1β signaling (22, 60, 62).

Transferred to a more clinical situation where β-cells are under inflammatory attack by a combination of different cytokines the picture will be even more complex. Considering that we are dealing with a dynamic network of protein-to-protein interactions, it is most probable that perturbations of this network, induced by the local inflammatory environment, will result in β-cell dysfunction and eventually apoptotic cell death, leading to a diabetic phenotype. Molecular chaperones are suggested to play a crucial role in maintaining this dynamic network, and the present data suggest that the balance between the post-translationally modified and unmodified forms of the chaperones may be of relevance for the cellular outcome. Other central players are the proteins involved in RNA metabolism, such as the hnRNPs and DEAD box proteins. Use of the novel tools for network analysis (28) provides evidence for protein-to-protein interactions between these central players on the one hand and many of the proteins involved in energy metabolism and cytoskeleton organization on the other hand (Fig. 6) that will have a major impact on β-cell function. These findings lead us to hypothesize that, although upon an inflammatory attack the β-cell will eventually die from apoptosis, many important alterations are taking place that will affect the homeostasis of the cell state, resulting in a global β-cell dysfunction. This is also evidenced by the major detrimental effects on insulin processing and secretion, which are after all the primary tasks of this highly specialized cell. In conclusion, the present findings provide new insights into the protein pathways triggered in β-cells undergoing an inflammatory attack, pointing to a crucial role for chaperones and proteins involved in RNA processing. Together with previously published studies (9), a more comprehensive knowledge of the complexity of the networks involved will make it possible to develop new strategies for the treatment of type 1 diabetes.

Acknowledgments—We gratefully acknowledge the technical experience of Dirk Valckx, Karin Schildermans, and Van Zon.

* This work was supported in part by the Catholic University of Leuven (Grants GOA 2004/10 and EF/05/007), the Flemish Research Foundation (Grants FWO G.0084.02 and G.0233.04, a postdoctoral fellowship to C. G. and G. V. d. B. and a clinical research fellowship to C. M.), the Belgium Program on Interuniversity Poles of Attraction initiated by the Belgian State (Grants IUAP P5/17 and P6/40), the European Union Project SAVEBETA (Contract 036903 in the Framework Program 6 of the European Community), and the Centre of Excellence SymBioSys (Research Council KULeuven Grant EF/05/007). The costs of publication of this article were defrayed in part by the payment of page charges. This article must therefore be hereby marked "*advertisement*" in accordance with 18 U.S.C. Section 1734 solely to indicate this fact.

S The on-line version of this article (available at http://www.mcponline.org) contains supplemental material.

[b] Both authors contributed equally to this work.

[c] To whom correspondence should be addressed: Laboratory for Experimental Medicine and Endocrinology, UZ-Gasthuisberg, Onderwijs en Navorsing, Herestraat 49, bus 902, B-3000 Leuven, Belgium. Tel.: 32-16-34-61-63; Fax: 32-16-34-60-35; E-mail lut.overbergh@med.kuleuven.be.

[f] A research associate of the Fonds National de la Recherche Scientifique (Belgium).

REFERENCES

1. Mathis, D., Vence, L., and Benoist, C. (2001) β-Cell death during progression to diabetes. *Nature* **414,** 792–798
2. Eizirik, D. L., and Mandrup-Poulsen, T. (2001) A choice of death—the signal-transduction of immune-mediated beta-cell apoptosis. *Diabetologia* **44,** 2115–2133
3. Cnop, M., Welsh, N., Jonas, J. C., Jorns, A., Lenzen, S., and Eizirik, D. L. (2005) Mechanisms of pancreatic β-cell death in type 1 and type 2 diabetes: many differences, few similarities. *Diabetes* **54,** Suppl. 2, S97–S107
4. Hostens, K., Pavlovic, D., Zambre, Y., Ling, Z., Van Schravendijk, C., Eizirik,

Molecular & Cellular Proteomics

Downloaded from www.mcponline.org by on January 2, 2008

D. L., and Pipeleers, D. G. (1999) Exposure of human islets to cytokines can result in disproportionately elevated proinsulin release. *J. Clin. Investig.* **104,** 67–72
5. Ohara-Imaizumi, M., Cardozo, A. K., Kikuta, T., Eizirik, D. L., and Nagamatsu, S. (2004) The cytokine interleukin-1β reduces the docking and fusion of insulin granules in pancreatic β-cells, preferentially decreasing the first phase of exocytosis. *J. Biol. Chem.* **279,** 41271–41274
6. Borjesson, A., and Carlsson, C. (2007) Altered proinsulin conversion in rat pancreatic islets exposed long-term to various glucose concentrations or interleukin-1β. *J. Endocrinol.* **192,** 381–387
7. Cardozo, A. K., Heimberg, H., Heremans, Y., Leeman, R., Kutlu, B., Kruhoffer, M., Orntoft, T., and Eizirik, D. L. (2001) A comprehensive analysis of cytokine-induced and nuclear factor-κB-dependent genes in primary rat pancreatic β-cells. *J. Biol. Chem.* **276,** 48879–48886
8. Delaney, C. A., Pavlovic, D., Hoorens, A., Pipeleers, D. G., and Eizirik, D. L. (1997) Cytokines induce deoxyribonucleic acid strand breaks and apoptosis in human pancreatic islet cells. *Endocrinology* **138,** 2610–2614
9. Kutlu, B., Cardozo, A. K., Darville, M. I., Kruhoffer, M., Magnusson, N., Orntoft, T., and Eizirik, D. L. (2003) Discovery of gene networks regulating cytokine-induced dysfunction and apoptosis in insulin-producing INS-1 cells. *Diabetes* **52,** 2701–2719
10. Papaccio, G., Graziano, A., D'Aquino, R., Valiante, S., and Naro, F. (2005) A biphasic role of nuclear transcription factor (NF)-κB in the islet β-cell apoptosis induced by interleukin (IL)-1β. *J. Cell Physiol.* **204,** 124–130
11. Gysemans, C. A., Ladriere, L., Callewaert, H., Rasschaert, J., Flamez, D., Levy, D. E., Matthys, P., Eizirik, D. L., and Mathieu, C. (2005) Disruption of the γ-interferon signaling pathway at the level of signal transducer and activator of transcription-1 prevents immune destruction of β-cells. *Diabetes* **54,** 2396–2403
12. Gygi, S. P., Rochon, Y., Franza, B. R., and Aebersold, R. (1999) Correlation between protein and mRNA abundance in yeast. *Mol. Cell. Biol.* **19,** 1720–1730
13. Apweiler, R., Hermjakob, H., and Sharon, N. (1999) On the frequency of protein glycosylation, as deduced from analysis of the SWISS-PROT database. *Biochim. Biophys. Acta* **1473,** 4–8
14. Mann, M., and Jensen, O. N. (2003) Proteomic analysis of post-translational modifications. *Nat. Biotechnol.* **21,** 255–261
15. Sparre, T., Christensen, U. B., Mose, L. P., Fey, S. J., Wrzesinski, K., Roepstorff, P., Mandrup-Poulsen, T., Pociot, F., Karlsen, A. E., and Nerup, J. (2002) IL-1β induced protein changes in diabetes prone BB rat islets of Langerhans identified by proteome analysis. *Diabetologia* **45,** 1550–1561
16. Sparre, T., Christensen, U. B., Gotfredsen, C. F., Larsen, P. M., Fey, S. J., Hjerno, K., Roepstorff, P., Pociot, F., Karlsen, A. E., and Nerup, J. (2004) Changes in expression of IL-1β influenced proteins in transplanted islets during development of diabetes in diabetes-prone BB rats. *Diabetologia* **47,** 892–908
17. Sparre, T., Larsen, M. R., Heding, P. E., Karlsen, A. E., Jensen, O. N., and Pociot, F. (2005) Unraveling the pathogenesis of type 1 diabetes with proteomics: present and future directions. *Mol. Cell. Proteomics* **4,** 441–457
18. Marouga, R., David, S., and Hawkins, E. (2005) The development of the DIGE system: 2D fluorescence difference gel analysis technology. *Anal. Bioanal. Chem.* **382,** 669–678
19. D'Hertog, W., Mathieu, C., and Overbergh, L. (2006) Type 1 diabetes: entering the proteomic era. *Expert Rev. Proteomics* **3,** 223–236
20. Tonge, R., Shaw, J., Middleton, B., Rowlinson, R., Rayner, S., Young, J., Pognan, F., Hawkins, E., Currie, I., and Davison, M. (2001) Validation and development of fluorescence two-dimensional differential gel electrophoresis proteomics technology. *Proteomics* **1,** 377–396
21. Merglen, A., Theander, S., Rubi, B., Chaffard, G., Wollheim, C. B., and Maechler, P. (2004) Glucose sensitivity and metabolism-secretion coupling studied during two-year continuous culture in INS-1E insulinoma cells. *Endocrinology* **145,** 667–678
22. Ortis, F., Cardozo, A. K., Crispim, D., Storling, J., Mandrup-Poulsen, T., and Eizirik, D. L. (2006) Cytokine-induced proapoptotic gene expression in insulin-producing cells is related to rapid, sustained, and nonoscillatory nuclear factor-κB activation. *Mol. Endocrinol.* **20,** 1867–1879
23. Hoorens, A., Van de Casteele, M., Kloppel, G., and Pipeleers, D. (1996) Glucose promotes survival of rat pancreatic β cells by activating synthesis of proteins which suppress a constitutive apoptotic program. *J. Clin. Investig.* **98,** 1568–1574
24. Green, L. C., Wagner, D. A., Glogowski, J., Skipper, P. L., Wishnok, J. S., and Tannenbaum, S. R. (1982) Analysis of nitrate, nitrite, and [^{15}N]nitrate in biological fluids. *Anal. Biochem.* **126,** 131–138
25. Bradford, M. M. (1976) A rapid and sensitive method for the quantitation of microgram quantities of protein utilizing the principle of protein-dye binding. *Anal. Biochem.* **72,** 248–254
26. Altschul, S. F., Madden, T. L., Schaffer, A. A., Zhang, J., Zhang, Z., Miller, W., and Lipman, D. J. (1997) Gapped BLAST and PSI-BLAST: a new generation of protein database search programs. *Nucleic Acids Res.* **25,** 3389–3402
27. Hinsby, A. M., Kiemer, L., Karlberg, E. O., Lage, K., Fausboll, A., Juncker, A. S., Andersen, J. S., Mann, M., and Brunak, S. (2006) A wiring of the human nucleolus. *Mol. Cell* **22,** 285–295
28. Lage, K., Karlberg, E. O., Storling, Z. M., Olason, P. I., Pedersen, A. G., Rigina, O., Hinsby, A. M., Tumer, Z., Pociot, F., Tommerup, N., Moreau, Y., and Brunak, S. (2007) A human phenome-interactome network of protein complexes implicated in genetic disorders. *Nat. Biotechnol.* **25,** 309–316
29. Li, D., and Roberts, R. (2001) WD-repeat proteins: structure characteristics, biological function, and their involvement in human diseases. *CMLS Cell. Mol. Life Sci.* **58,** 2085–2097
30. DesMarais, V., Ghosh, M., Eddy, R., and Condeelis, J. (2005) Cofilin takes the lead. *J. Cell Sci.* **118,** 19–26
31. Dan, C., Kelly, A., Bernard, O., and Minden, A. (2001) Cytoskeletal changes regulated by the PAK4 serine/threonine kinase are mediated by LIM kinase 1 and cofilin. *J. Biol. Chem.* **276,** 32115–32121
32. Grantham, J., Ruddock, L. W., Roobol, A., and Carden, M. J. (2002) Eukaryotic chaperonin containing T-complex polypeptide 1 interacts with filamentous actin and reduces the initial rate of actin polymerization in vitro. *Cell Stress Chaperones* **7,** 235–242
33. Verboven, C., Bogaerts, I., Waelkens, E., Rabijns, A., Van Baelen, H., Bouillon, R., and De Ranter, C. (2003) Actin-DBP: the perfect structural fit? *Acta Crystallogr. Sect. D Biol. Crystallogr.* **59,** 263–273
34. Hansen, B. S., Nielsen, J. H., Linde, S., Spinas, G. A., Welinder, B. S., Mandrup-Poulsen, T., and Nerup, J. (1988) Effect of interleukin-1 on the biosynthesis of proinsulin and insulin in isolated rat pancreatic islets. *Biomed. Biochim. Acta* **47,** 305–309
35. Lee, K. K., Murakawa, M., Takahashi, S., Tsubuki, S., Kawashima, S., Sakamaki, K., and Yonehara, S. (1998) Purification, molecular cloning, and characterization of TRP32, a novel thioredoxin-related mammalian protein of 32 kDa. *J. Biol. Chem.* **273,** 19160–19166
36. Laybutt, D. R., Preston, A. M., Akerfeldt, M. C., Kench, J. G., Busch, A. K., Biankin, A. V., and Biden, T. J. (2007) Endoplasmic reticulum stress contributes to beta cell apoptosis in type 2 diabetes. *Diabetologia* **50,** 752–763
37. Nagano, K., Masters, J. R., Akpan, A., Yang, A., Corless, S., Wood, C., Hastie, C., Zvelebil, M., Cramer, R., and Naaby-Hansen, S. (2004) Differential protein synthesis and expression levels in normal and neoplastic human prostate cells and their regulation by type I and II interferons. *Oncogene* **23,** 1693–1703
38. Pirot, P., Eizirik, D. L., and Cardozo, A. K. (2006) Interferon-γ potentiates endoplasmic reticulum stress-induced death by reducing pancreatic beta cell defence mechanisms. *Diabetologia* **49,** 1229–1236
39. Freiden, P. J., Gaut, J. R., and Hendershot, L. M. (1992) Interconversion of three differentially modified and assembled forms of BiP. *EMBO J.* **11,** 63–70
40. Hendershot, L. M., Ting, J., and Lee, A. S. (1988) Identity of the immunoglobulin heavy-chain-binding protein with the 78,000-dalton glucose-regulated protein and the role of posttranslational modifications in its binding function. *Mol. Cell. Biol.* **8,** 4250–4256
41. Hendershot, L. M. (2004) The ER function BiP is a master regulator of ER function. *Mt. Sinai J. Med.* **71,** 289–297
42. Nakatani, Y., Kaneto, H., Kawamori, D., Yoshiuchi, K., Hatazaki, M., Matsuoka, T. A., Ozawa, K., Ogawa, S., Hori, M., Yamasaki, Y., and Matsuhisa, M. (2005) Involvement of endoplasmic reticulum stress in insulin resistance and diabetes. *J. Biol. Chem.* **280,** 847–851
43. Wu, S. J., Liu, F. H., Hu, S. M., and Wang, C. (2001) Different combinations of the heat-shock cognate protein 70 (hsc70) C-terminal functional groups are utilized to interact with distinct tetratricopeptide repeat-containing proteins. *Biochem. J.* **359,** 419–426

Molecular & Cellular Proteomics

Downloaded from www.mcponline.org by on January 2, 2008

44. Lasunskaia, E. B., Fridlianskaia, I. I., Guzhova, I. V., Bozhkov, V. M., and Margulis, B. A. (1997) Accumulation of major stress protein 70kDa protects myeloid and lymphoid cells from death by apoptosis. *Apoptosis* **2,** 156–163
45. John, N. E., Andersen, H. U., Fey, S. J., Larsen, P. M., Roepstorff, P., Larsen, M. R., Pociot, F., Karlsen, A. E., Nerup, J., Green, I. C., and Mandrup-Poulsen, T. (2000) Cytokine- or chemically derived nitric oxide alters the expression of proteins detected by two-dimensional gel electrophoresis in neonatal rat islets of Langerhans. *Diabetes* **49,** 1819–1829
46. Jolly, C., and Morimoto, R. I. (2000) Role of the heat shock response and molecular chaperones in oncogenesis and cell death. *J. Natl. Cancer Inst.* **92,** 1564–1572
47. Wadhwa, R., Takano, S., Kaur, K., Deocaris, C. C., Pereira-Smith, O. M., Reddel, R. R., and Kaul, S. C. (2006) Upregulation of mortalin/mthsp70/Grp75 contributes to human carcinogenesis. *Int. J. Cancer* **118,** 2973–2980
48. Bast, A., Wolf, G., Oberbaumer, I., and Walther, R. (2002) Oxidative and nitrosative stress induces peroxiredoxins in pancreatic beta cells. *Diabetologia* **45,** 867–876
49. Kang, S. W., Chae, H. Z., Seo, M. S., Kim, K., Baines, I. C., and Rhee, S. G. (1998) Mammalian peroxiredoxin isoforms can reduce hydrogen peroxide generated in response to growth factors and tumor necrosis factor-α. *J. Biol. Chem.* **273,** 6297–6302
50. Thiede, B., Siejak, F., Dimmler, C., and Rudel, T. (2002) Prediction of translocation and cleavage of heterogeneous ribonuclear proteins and Rho guanine nucleotide dissociation inhibitor 2 during apoptosis by subcellular proteome analysis. *Proteomics* **2,** 996–1006
51. Bomsztyk, K., Van Seuningen, I., Suzuki, H., Denisenko, O., and Ostrowski, J. (1997) Diverse molecular interactions of the hnRNP K protein. *FEBS Lett.* **403,** 113–115
52. Chang, P. C., Chi, C. W., Chau, G. Y., Li, F. Y., Tsai, Y. H., Wu, J. C., and Wu Lee, Y. H. (2006) DDX3, a DEAD box RNA helicase, is deregulated in hepatitis virus-associated hepatocellular carcinoma and is involved in cell growth control. *Oncogene* **25,** 1991–2003
53. Cardozo, A. K., Kruhoffer, M., Leeman, R., Orntoft, T., and Eizirik, D. L. (2001) Identification of novel cytokine-induced genes in pancreatic β-cells by high-density oligonucleotide arrays. *Diabetes* **50,** 909–920
54. Eizirik, D. L., Kutlu, B., Rasschaert, J., Darville, M., and Cardozo, A. K. (2003) Use of microarray analysis to unveil transcription factor and gene networks contributing to β cell dysfunction and apoptosis. *Ann. N. Y. Acad. Sci.* **1005,** 55–74
55. Rasschaert, J., Liu, D., Kutlu, B., Cardozo, A. K., Kruhoffer, M., Orntoft, T. F., and Eizirik, D. L. (2003) Global profiling of double stranded RNA- and IFN-γ-induced genes in rat pancreatic beta cells. *Diabetologia* **46,** 1641–1657
56. Ylipaasto, P., Kutlu, B., Rasilainen, S., Rasschaert, J., Salmela, K., Teerijoki, H., Korsgren, O., Lahesmaa, R., Hovi, T., Eizirik, D. L., Otonkoski, T., and Roivainen, M. (2005) Global profiling of coxsackievirus- and cytokine-induced gene expression in human pancreatic islets. *Diabetologia* **48,** 1510–1522
57. Cardozo, A. K., Proost, P., Gysemans, C., Chen, M. C., Mathieu, C., and Eizirik, D. L. (2003) IL-1β and IFN-γ induce the expression of diverse chemokines and IL-15 in human and rat pancreatic islet cells, and in islets from pre-diabetic NOD mice. *Diabetologia* **46,** 255–266
58. Rasschaert, J., Ladriere, L., Urbain, M., Dogusan, Z., Katabua, B., Sato, S., Akira, S., Gysemans, C., Mathieu, C., and Eizirik, D. L. (2005) Toll-like receptor 3 and STAT-1 contribute to double-stranded RNA+ interferon-γ-induced apoptosis in primary pancreatic β-cells. *J. Biol. Chem.* **280,** 33984–33991
59. Larsen, C. M., Faulenbach, M., Vaag, A., Volund, A., Ehses, J. A., Seifert, B., Mandrup-Poulsen, T., and Donath, M. Y. (2007) Interleukin-1-receptor antagonist in type 2 diabetes mellitus. *N. Engl. J. Med.* **356,** 1517–1526
60. Maedler, K., Schumann, D. M., Sauter, N., Ellingsgaard, H., Bosco, D., Baertschiger, R., Iwakura, Y., Oberholzer, J., Wollheim, C. B., Gauthier, B. R., and Donath, M. Y. (2006) Low concentration of interleukin-1β induces FLICE-inhibitory protein-mediated β-cell proliferation in human pancreatic islets. *Diabetes* **55,** 2713–2722
61. Welsh, N., Cnop, M., Kharroubi, I., Bugliani, M., Lupi, R., Marchetti, P., and Eizirik, D. L. (2005) Is there a role for locally produced interleukin-1 in the deleterious effects of high glucose or the type 2 diabetes milieu to human pancreatic islets? *Diabetes* **54,** 3238–3244
62. Hoorens, A., Stange, G., Pavlovic, D., and Pipeleers, D. (2001) Distinction between interleukin-1-induced necrosis and apoptosis of islet cells. *Diabetes* **50,** 551–557

Molecular & Cellular Proteomics

Downloaded from www.mcponline.org by on January 2, 2008